arXiv:2607.15621v1 [cs.RO] 17 Jul 2026

Think at 5 Hz, Act at 20 Hz: Asynchronous Fast-Slow Vision-Language-Action Inference for Closed-Loop Driving

Yun Li[1], Jiachen Gong[1], Simon Thompson[2], Ehsan Javanmardi[1], Qunli Zhang[3], Zifan Zeng[3], Shiming Liu[3], Peng Wang[3], Zixuan Guo[1], and Manabu Tsukada[1]

[1] The University of Tokyo, Tokyo, Japan
li-yun@g.ecc.u-tokyo.ac.jp
[2] TIER IV, Inc., Tokyo, Japan
[3] Huawei

Abstract. Large language models bring instruction following and scene reasoning to end-to-end driving, but their inference latency collides with the control rate a vehicle requires. Existing closed-loop agents hide this gap by invoking the model on alternate simulation ticks and replaying the previous command in between, so half of all control outputs ignore the newest observations. We present a fast-slow architecture that removes this compromise. A frozen 7B vision-language backbone acts as the slow system, digesting navigation instructions and visual history at low frequency while exposing its per-layer key-value cache as a standing representation of the scene. A lightweight action expert acts as the fast system, attending to this cache and to the current camera frame at every simulation tick to regress waypoints in a single forward pass. Since the cache lags behind the world at deployment, we train the expert under randomized staleness, aligning training with asynchronous execution. On LangAuto-Short routes in CARLA, our system produces fresh control at every 50 ms simulation tick and lifts route completion from 37.0 to 94.0 over the frame-skipping baseline. A frame-skip ablation with the same expert separates the two factors at work: the expert raises the driving score on its own, while per-tick freshness raises completion from 82.1 to 94.0 and cuts red-light violations by a third. Trained on a single town, the expert transfers zero-shot to two unseen towns, holding 84–94% route completion where the baseline reaches 31–41%. It reduces open-loop waypoint error by nearly a factor of four compared to the backbone's own action head, at a per-tick model cost of 32 ms that is independent of history length on a single consumer GPU.

Keywords: Vision-language-action models · Autonomous driving · Real-time inference

1 Introduction

Language-conditioned driving agents built on large vision-language models follow natural-language navigation instructions, explain their decisions, and inherit

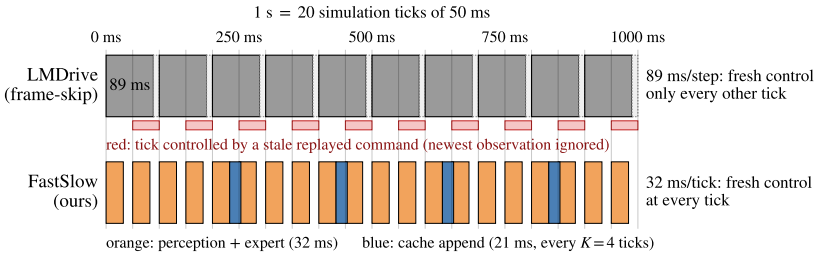

Fig. 1: One second of control under the two schedules, at the measured per-stage latencies of Table 3. The frame-skipping agent spends 89 ms per invocation, so it produces fresh control only at every other 50 ms tick and replays a stale command in between. Our expert reads the backbone's cached context and issues fresh control at every tick for 32 ms, plus a 21 ms cache append every K=4 ticks.

world knowledge from internet-scale pretraining [16,19,24]. The price of this capability is inference cost. A 7B backbone that re-reads its full visual history at every control step cannot keep up with the 20 Hz tick rate of a closed-loop simulator, let alone a real vehicle. The canonical open-source agent of this family, LMDrive [16], resolves the conflict by running its model on every second tick and replaying the stale control command in between. Half of the time, the vehicle acts on a decision that ignores the most recent 50–100 ms of observation.

We argue that the latency problem is architectural, not fundamental. Instruction understanding and temporal scene aggregation, the expensive parts of a VLA agent, change slowly, while mapping the current frame to a trajectory must happen quickly yet is computationally light. This observation suggests a fast-slow decomposition (Figure 2) in the spirit of dual-process designs explored for driving by DriveVLM [20] and for manipulation by π_0 [1].

Recent work on action experts, notably DriveVLA-W0 [8], pairs a large VLA backbone with a small decoder through joint attention, but evaluates only open-loop planning benchmarks where all computation is synchronous and latency is measured rather than lived. Whether a fast-slow VLA can absorb cache staleness and still improve driving outcomes at full control rate on commodity hardware has not been demonstrated.

This paper provides that demonstration. We attach a 337M-parameter action expert to a frozen LMDrive backbone. Every layer of the expert projects its tokens into the backbone's attention space and cross-attends into the backbone's per-layer key-value cache; the backbone never attends back, so the cache evolves exactly as it would alone. This asymmetry enables asynchronous deployment. The slow system appends one frame to its cache every K ticks as an incremental four-token forward pass, rebuilding the cache only when the instruction, a runtime notice, or an episode boundary invalidates it, while the fast system reads whatever cache exists at every tick. Because the cache the expert reads lags the world by up to K ticks, we train the expert under randomized staleness, truncating the backbone prefix visible to each supervised frame by a random number

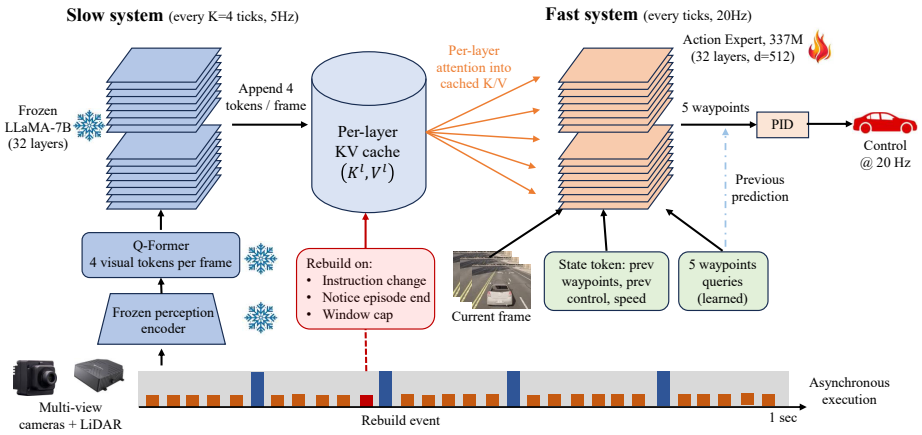

Fig. 2: Asynchronous fast-slow inference. The frozen backbone (left) digests instruction and history every K ticks, appending four tokens per frame to its per-layer KV cache through an incremental forward pass; the cache is rebuilt only on invalidation events. The action expert (right) runs at every simulation tick: its ten tokens cross-attend into the cached keys and values at each of the 32 layers and regress five waypoints. The backbone never attends to expert tokens, so the cache is identical with or without the expert.

of frames so the expert must compensate through the current frame and an ego-state token that carries its own previous prediction. A golden equivalence test confirms that incremental caching is numerically faithful, since switching from monolithic to incremental prefill moves predicted waypoints by less than 4 mm.

On the LangAuto-Short benchmark in CARLA [4], our agent issues fresh control at every simulation tick on a single RTX 3090 Ti and lifts the driving score from 28.8 to 32.9 while raising route completion from 37.0 to 94.0 (two runs per configuration). A frame-skip ablation running the same expert at the baseline's 10 Hz cadence attributes the driving-score gain to the expert itself, and the completion gain, the near-elimination of route deviations and timeouts, and a third fewer red-light violations to per-tick freshness. Per-tick operation is itself available only through the cache: any head attached to a backbone that recomputes its history spends 89–169 ms per step and must skip frames to fit the budget. In open loop, the expert reduces validation waypoint L1 error from 0.123 to 0.031, nearly a factor of four below the frozen backbone's own action head, with only 337M trained parameters and five epochs of training on a single GPU. Ablations isolate the contribution of staleness augmentation, which improves validation waypoint error at every training epoch and ends at 0.031 against 0.037 for a δ=0-only twin.

We make three contributions. We introduce an asynchronous fast-slow inference scheme for VLA driving that turns the backbone into a cached, incrementally updated context provider and moves all per-tick computation into a lightweight expert. We propose staleness-augmented training, which aligns the

training distribution with the asynchronous deployment distribution. We present the first closed-loop evaluation of the fast-slow VLA paradigm under measured latency on consumer hardware.

2 Related Work

Language-guided end-to-end driving. Sensor-fusion policies that operate without any language interface, including TransFuser [3, 12], InterFuser [17], TCP [22], and ReasonNet [18], remain strong closed-loop baselines on CARLA, so a language-guided system must justify the latency of its reasoning stack. Coupling driving policies to language models began with interpretability — DriveGPT4 [24] narrates and predicts controls, DriveLM [19] structures scene understanding as graph question answering — and matured into closed-loop instruction following with LMDrive [16], which drives in CARLA from natural-language commands and multi-modal sensor streams. GPT-Driver [9] recasts motion planning as language modeling, Agent-Driver [10] surrounds the planner with tool use and memory, and EMMA [5] maps camera input directly to trajectories, but these are evaluated open-loop on recorded logs where inference latency carries no penalty. Vision-only successors such as CarLLaVA [15] and SimLingo [14] raised closed-loop benchmark scores while keeping the full language model inside the control loop. None of these systems addresses the resulting rate mismatch; in practice their public agents throttle the simulator or replay stale commands between model invocations. Our work keeps the LMDrive stack intact and changes only where computation happens in time.

Fast-slow architectures and action experts. Dual-process designs separate deliberate reasoning from fast reaction. DriveVLM [20] pairs a VLM planner with a classical trajectory refiner, but the two subsystems exchange only trajectories; the fast path never sees the slow system's internal representation. In manipulation, π_0 [1] couples a VLM with a flow-matching action expert through joint attention inside one synchronous forward pass, and action-chunking policies such as ACT [25], Diffusion Policy [2], and $\pi_{0.5}$ [11] decouple decision rate from control rate by emitting several future actions per inference call. DriveVLA-W0 [8] brings this coupling to driving and shows that an asymmetric variant in which the backbone never attends to expert tokens preserves planning quality on NAVSIM, yet both training and evaluation remain synchronous and open-loop. We take the asymmetry to its logical conclusion. Since the backbone's computation is independent of the expert, its key-value cache can be reused across many expert invocations, which turns the synchronous coupling into an asynchronous fast-slow system with the backbone's per-layer cache as the interface. The expert must now tolerate stale context, which we address with randomized staleness, and the evaluation can close the loop under measured latency on consumer hardware.

Efficient inference for control. Key-value caching and incremental decoding are standard machinery for autoregressive text generation, and robotics has begun to exploit them for real-time action chunking [1]. Acting on inputs that lag the world is a classical concern in control, studied as Markov decision processes with observation and action delays [6], and reinforcement learning has revisited the setting by letting the environment evolve while the agent computes [13, 23]. Staleness-augmented training is the imitation-learning counterpart of these ideas for a cached context. Orthogonal strategies such as distillation, quantization, and speculative decoding shrink or parallelize the model itself. We instead reorganize when each component runs, leaving the backbone neither compressed nor retrained and moving the entire per-tick budget into a 337M expert whose cost is independent of history length.

3 Method

Figure 2 gives an overview. We build on LMDrive [16]. A frozen perception encoder converts multi-view camera images and LiDAR into per-frame features, a Q-Former [7] compresses each frame into n=4 visual tokens conditioned on the instruction, and a frozen LLaMA-7B backbone [21] consumes the token sequence $[\,\text{text} \mid f_1 \mid f_2 \mid \cdots]$, optionally with a runtime notice inserted mid-sequence. The original agent regresses waypoints from the backbone's final hidden states with a small MLP head and recomputes the entire sequence at every invocation.

3.1 Action Expert with Per-Layer Cache Attention

The expert is a 32-layer transformer with hidden width d_{ae}=512, matched one-to-one with backbone layers. At layer ℓ it forms queries, keys, and values from its own tokens through rectangular projections $W^{\ell}_{q,k,v} \in \mathbb{R}^{4096\times 512}$ into the backbone's 32-head, 128-dimensional attention geometry, concatenates the backbone's cached keys and values of the same layer, and performs a single attention operation

$$\text{Attn}\big(Q^{\ell}_{\text{ae}},\ [K^{\ell}_{\text{vlm}}; K^{\ell}_{\text{ae}}],\ [V^{\ell}_{\text{vlm}}; V^{\ell}_{\text{ae}}]\big)\,, \tag{1}$$

followed by an output projection back to d_{ae} and a SwiGLU feed-forward block. The backbone never attends to expert tokens, so the cached $K_{\text{vlm}}, V_{\text{vlm}}$ are identical whether or not the expert runs, the property that permits caching. Expert tokens carry learned positional embeddings and no rotary encoding, following the design validated by DriveVLA-W0 [8]; backbone keys retain the rotary phases they were cached with.

Per frame the expert consumes ten tokens: one state token embedding the previous predicted waypoints, the previous control triplet, current speed, and the target point; the current frame's four visual tokens, produced by the same Q-Former pipeline the backbone uses; and five learnable waypoint queries, decoded to five (x, y) waypoints by a two-layer head under L1 supervision. The expert totals 337M parameters. The backbone, Q-Former, and original heads stay frozen, so training builds no autograd graph through the 7B model and peaks below 28 GB of GPU memory at batch size four.

Fig. 3: The four evaluation towns. The expert is trained on short routes from town05 only; towns 01, 02, and 03 are never seen during expert training, and town03 is evaluated on the long-route tier.

3.2 Staleness-Augmented Training

At deployment the cache lags the current frame by up to K ticks. We replicate this gap during training by drawing $\delta \sim \mathcal{U}\{0, \ldots, \delta_{\max}\}$ for each sample and masking the backbone prefix visible to frame j's expert block so that it ends at frame $j - \delta$, or at the instruction text alone when $j < \delta$. The expert therefore learns to fuse an outdated scene summary with fresh per-tick evidence. The state token is trained with teacher-forced previous waypoints under Gaussian noise and random dropout, limiting exposure bias. All frames of a training clip are supervised in parallel through per-block attention masks, which reproduces the cache visibility of per-frame deployment while leaving the data pipeline untouched, since the previous-action fields the state token needs already exist in LMDrive's driving logs.

3.3 Asynchronous Deployment

The agent maintains the backbone cache as mutable state. Every K=4 ticks (0.2 s at 20 Hz, matching the training frame grid) the current frame's four tokens are appended through an incremental forward pass whose cost is independent of history length; the episode-boundary classifier runs on the resulting hidden states. The cache is rebuilt from scratch only on instruction change, notice arrival, episode end, or when the cached history reaches the training window cap. At every tick the expert reads the cache as-is, so test-time staleness is bounded by $K-1$ ticks and stays inside the training distribution. Rotary phases make append-only caching exact. A golden test comparing monolithic against incremental prefill confirms this, with waypoint differences below 4 mm at the fp16 noise floor.

4 Experiments

4.1 Setup

We train on the town05 portion of the LMDrive corpus: 27,485 instruction clips of up to 40 frames, with three weather conditions held out for validation. The expert trains for five epochs on one 48 GB GPU with AdamW, a cosine schedule from 10^{-4}, and an effective batch size of 32; the backbone, perception encoder,

Table 1: Validation waypoint L1 (m) on held-out weathers, all evaluated under the synchronous δ=0 protocol with teacher-forced state tokens.

Method	L1 ↓	Params trained
Backbone action head (frozen)	0.123	—
Action expert, δ=0 only	0.037	337M
Action expert, randomized δ (ours)	**0.031**	337M

Table 2: LangAuto-Short, town05, 32 routes, identical simulator settings. DS: driving score; RC: route completion; IS: infraction score. Baseline and ours are means ± half-range over two independent runs each; the frame-skipped middle row runs the same trained expert at the baseline's 10 Hz replay cadence (single run) and isolates control freshness from expert quality.

Agent	Control rate	DS ↑	RC ↑	IS ↑
LMDrive (replayed ticks)	10 Hz	28.8 ± 0.8	37.0 ± 0.4	$\mathbf{0.80} \pm 0.04$
FastSlow-LMDrive, frame-skipped	10 Hz	**34.0**	82.1	0.45
FastSlow-LMDrive (ours)	20 Hz	32.9 ± 0.7	$\mathbf{94.0} \pm 2.6$	0.37 ± 0.02

Q-Former, and original heads stay frozen throughout, initialized from the public LMDrive checkpoint. Closed-loop evaluation uses the 32 LangAuto-Short town05 routes in CARLA 0.9.10 on a single RTX 3090 Ti, with identical simulator settings, scenario definitions, and PID parameters for every agent; the baseline is the public LMDrive agent, which invokes its model on alternate ticks and replays the previous command otherwise. We report the standard driving score, route completion, and infraction score, plus per-stage latency measured both in a controlled sweep over history lengths and inside the running loop.

4.2 Open-Loop Waypoint Accuracy

All rows share the synchronous δ=0 protocol, in which the state token receives teacher-forced previous waypoints, an input the frozen backbone head does not consume; part of the open-loop gap therefore reflects this privileged signal. The closed-loop comparison below, where the expert sees only its own predictions, confirms the gain without teacher forcing.

4.3 Closed-Loop Driving

The completion gap dominates the comparison. The baseline accumulates 25.0 route deviations and 2.9 timeouts per kilometer, symptoms of acting on stale decisions, against 4.3 and 0.08 for ours (two-run means). Our infraction score is lower, and exposure explains only part of it. A vehicle that completes 2.5 times more route meets traffic the baseline never reaches, but distance normalization does not remove the gap, since per-kilometer vehicle collisions still rise from 3.2 to

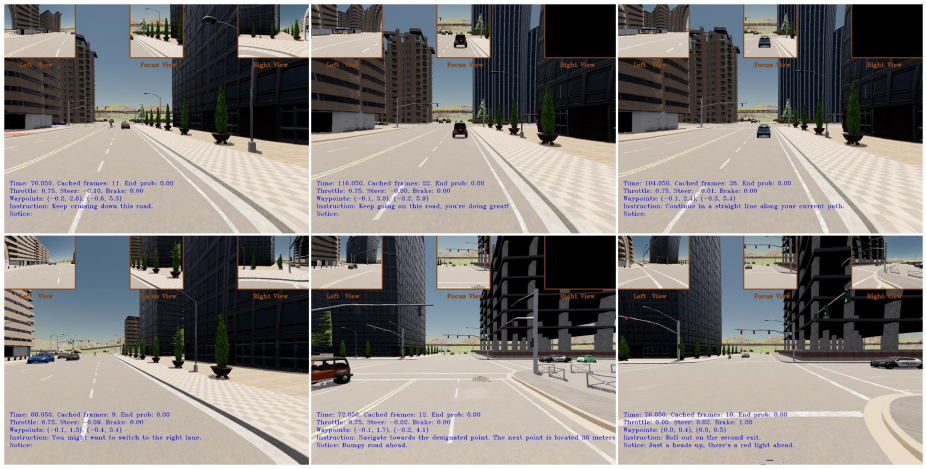

Fig. 4: Closed-loop driving in town05. Each panel shows the forward view with side views, the active navigation instruction, the runtime notice, and the predicted waypoints; the bottom-right panel brakes for a red light flagged by a notice.

11.2; the expert completes routes through traffic it has not learned to negotiate safely, a trade-off we revisit in the transfer experiments and the limitations. Infractions tied to inattention move the other way, with layout collisions dropping from 10.3 to 2.2 per kilometer and off-lane driving from 7.9 to 1.1. The low-level PID controller is reused from the 10 Hz baseline without retuning.

The frame-skipped middle row of Table 2 separates the two ingredients. Running the identical trained expert at the baseline's 10 Hz replay cadence already reaches a driving score of 34.0, so the driving-score improvement over the baseline traces to the expert rather than to control freshness. Freshness contributes elsewhere. Moving from 10 Hz to 20 Hz raises completion from 82.1 to 94.0, cuts route deviations from 11.3 to 4.3 per kilometer, reduces timeouts from 1.3 to 0.08, and lowers red-light violations from 10.4 to 6.9, while the added exposure costs infraction score (0.45 to 0.37) and leaves the composite driving score within run-to-run spread. The two rows are not equally available designs, however. Without cache reuse every step costs 89–169 ms (Table 3), so frame-skipping is the only form in which a recompute-based system fits the 50 ms budget; the cached 32 ms path is what makes the 20 Hz row feasible at all.

4.4 Latency

Figure 5 (left) shows the scaling. Legacy cost grows with history, from 59 ms at 10 frames to 169 ms at 100, because every step re-encodes everything the agent has seen, which is why the public agent skips ticks. Our per-tick model cost is flat. The expert reads the cache through attention dominated by its own ten tokens and measures 7–9 ms regardless of history length, while cache maintenance adds an amortized 5 ms per tick and full rebuilds (11 ms median in the loop) occur

Table 3: Per-stage latency (ms, median, RTX 3090 Ti) at a 40-frame history. Legacy recomputes Q-Former and backbone over the full history each step; ours touches the history only through the cache. In parentheses: medians measured inside the closed loop over 9,542 ticks. Totals are measured end to end rather than summed from stages; the in-loop agent step includes sensor formatting and harness overhead outside the model.

Stage	Legacy per step	Ours per tick	Ours per K=4 ticks
Perception + Q-Former	26.9	24.8 (29.2)	—
Backbone full recompute	61.6	—	—
Incremental append	—	—	21.1 (10.7)
Action expert	—	7.5 (9.3)	—
Total model compute	88.6	32.4	5.3 amortized
Total agent step, in loop	—	58	—

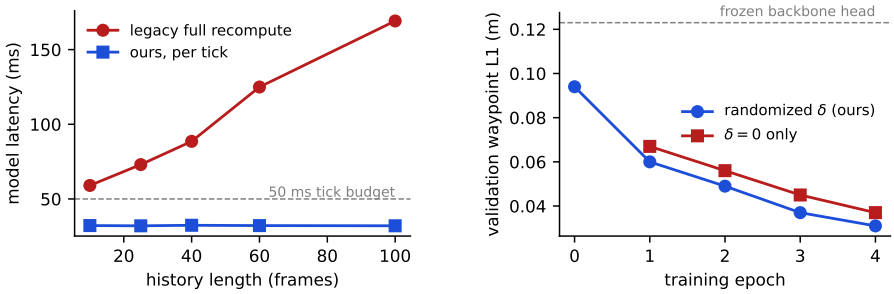

Fig. 5: Left: per-step model latency versus history length. The legacy path re-encodes the full history each step and exceeds the 50 ms tick budget at every history length, while our per-tick cost stays flat at 32 ms. Right: validation waypoint L1 across training epochs; the randomized-δ expert leads its δ=0 twin at every epoch and both leave the frozen backbone head far behind.

only at instruction changes, notices, and episode boundaries. Model compute thus stays approximately 18 ms below the 50 ms tick budget. The measured end-to-end agent step is 58 ms at the median, with the difference coming from sensor formatting and evaluation-harness overhead we did not optimize; in CARLA's synchronous mode the vehicle still receives fresh control at every tick, and the wall-clock rate is about 17 Hz.

4.5 Zero-Shot Town Transfer

The expert trains on town05 only, so evaluation on town01 and town02, layouts it has never seen, separates cache-reading skill from town memorization. The perception encoder, Q-Former, and backbone were pretrained on every town and are held fixed for both agents; zero-shot refers strictly to the 337M expert.

Table 4: Zero-shot transfer to unseen towns, single run per agent and town. The expert was trained on town05 only.

Town	Agent	Control rate	DS ↑	RC ↑	IS ↑
town01 (23 routes)	LMDrive	10 Hz	20.5	40.5	**0.56**
	FastSlow-LMDrive	20 Hz	**23.2**	**84.3**	0.26
town02 (15 routes)	LMDrive	10 Hz	11.6	30.7	**0.38**
	FastSlow-LMDrive	20 Hz	**28.3**	**94.4**	0.29

Route completion transfers almost intact, reaching 94.4 on town02 and 84.3 on town01 against 94.0 in-domain, which indicates that the expert has learned to read the backbone's cache and the current frame rather than a particular town's geometry. The advantage over the baseline persists in both unseen towns and is largest where the baseline degrades most, with 2.4 times its driving score and 3.1 times its completion on town02. Stale control appears to hurt most where the scene is unfamiliar.

Long-route transfer probes the boundary. We also evaluated eight LangAuto-Long routes in town03, several kilometers each, a tier absent from the expert's short-route training. Neither agent attains a usable driving score there. The baseline barely progresses, completing 12.7% of route on average for a 5.98 driving score earned largely by standing still, while ours completes 85.4% but accumulates enough vehicle collisions and red-light violations to collapse its penalty factor to 0.04, for a 2.96 driving score. Completion therefore transfers even to this tier, while hazard negotiation over long horizons does not. This points at the training data rather than the architecture, since short town05 clips contain few dense-traffic signalized encounters; long-route training clips are the natural next step.

4.6 Ablations

Staleness augmentation. Randomized-δ training improves accuracy even when no staleness is present at test time. Evaluated under the same synchronous protocol (δ=0), the randomized expert leads its δ=0-only twin at every epoch (0.060 versus 0.067, then 0.049 versus 0.056, 0.037 versus 0.045, and 0.031 versus 0.037 at convergence), so the augmentation regularizes even before staleness enters the picture. At deployment the δ=0 model additionally faces cache lag it never saw during training on three of every four ticks.

Limitations. Ours is a simulation study trained on short routes from one town. Hazard negotiation on long routes does not transfer, per-kilometer vehicle collisions increase alongside completion, the low-level controller inherits gains tuned for the slower baseline, and the main comparison covers two runs per configuration, with single runs for the frame-skip ablation and the transfer rows and

an observed run-to-run spread of up to 1.6 DS. A driving system requires safety validation far beyond a simulated benchmark, and nothing here should be read as evidence of road readiness.

5 Conclusion

Language models earn their place in a driving stack through understanding, and an architecture should not also demand reaction speed from the same component. We decomposed a language-guided driving agent along this line, pairing a frozen 7B backbone that maintains an incrementally cached representation of instruction and history with a 337M action expert that reads this cache through per-layer attention at every simulation tick. Randomized staleness during training aligns the expert with the asynchronous cache it meets at deployment, and closed-loop evaluation in CARLA shows that the two halves of the decomposition contribute separately: the expert lifts the driving score, and per-tick freshness, affordable only because the cache holds model cost flat regardless of history length, lifts route completion to 2.5 times the frame-skipping baseline. Limitations are cataloged alongside the experiments. The cache interface also opens directions we have not pursued here, from pretraining the backbone with world models to enrich what the cache encodes to using fast-slow disagreement as a training-free trigger for runtime safety supervision.

References

1. Black, K., Brown, N., Driess, D., Esmail, A., Equi, M., Finn, C., Fusai, N., Groom, L., Hausman, K., Ichter, B., Jakubczak, S., Jones, T., Ke, L., Levine, S., Li-Bell, A., Mothukuri, M., Nair, S., Pertsch, K., Shi, L.X., Tanner, J., Vuong, Q., Walling, A., Wang, H., Zhilinsky, U.: π_0: A vision-language-action flow model for general robot control. In: Robotics: Science and Systems 2025 (21 Jun 2025). https://doi.org/10.48550/arXiv.2410.24164, http://dx.doi.org/10.48550/arXiv.2410.24164 2, 4, 5
2. Chi, C., Feng, S., Du, Y., Xu, Z., Cousineau, E., Burchfiel, B., Song, S.: Diffusion policy: Visuomotor policy learning via action diffusion. In: Robotics: Science and Systems XIX. Robotics: Science and Systems Foundation (10 Jul 2023). https://doi.org/10.15607/rss.2023.xix.026, http://dx.doi.org/10.15607/rss.2023.xix.026 4
3. Chitta, K., Prakash, A., Jaeger, B., Yu, Z., Renz, K., Geiger, A.: TransFuser: Imitation with transformer-based sensor fusion for autonomous driving. IEEE Trans. Pattern Anal. Mach. Intell. **45**(11), 12878–12895 (Nov 2023). https://doi.org/10.1109/TPAMI.2022.3200245, http://dx.doi.org/10.1109/TPAMI.2022.3200245 4
4. Dosovitskiy, A., Ros, G., Codevilla, F., Lopez, A., Koltun, V.: CARLA: An Open Urban Driving Simulator. In: Levine, S., Vanhoucke, V., Goldberg, K. (eds.) Proceedings of the 1st Annual Conference on Robot Learning. Proceedings of Machine Learning Research, vol. 78, pp. 1–16. PMLR (2017), https://proceedings.mlr.press/v78/dosovitskiy17a.html 3

5. Hwang, J.J., Xu, R., Lin, H., Hung, W.C., Ji, J., Choi, K., Huang, D., He, T., Covington, P., Sapp, B., Zhou, Y., Guo, J., Anguelov, D., Tan, M.: EMMA: End-to-end Multimodal Model for autonomous driving. Transactions on Machine Learning Research (07/2025) (23 Jul 2025). https://doi.org/10.48550/arXiv.2410.23262, https://openreview.net/forum?id=kH3t5lmOU8 4
6. Katsikopoulos, K.V., Engelbrecht, S.E.: Markov decision processes with delays and asynchronous cost collection. IEEE Trans. Automat. Contr. **48**(4), 568–574 (Apr 2003). https://doi.org/10.1109/tac.2003.809799, http://dx.doi.org/10.1109/TAC.2003.809799 5
7. Li, J., Li, D., Savarese, S., Hoi, S.: BLIP-2: Bootstrapping language-image pre-training with frozen image encoders and large language models. In: International Conference on Machine Learning. arXiv (2023). https://doi.org/10.48550/ARXIV.2301.12597 5
8. Li, Y., Shang, S., Liu, W., Zhan, B., Wang, H., Wang, Y., Chen, Y., Wang, X., An, Y., Tang, C., Hou, L., Fan, L., Zhang, Z.: DriveVLA-W0: World models amplify data scaling law in autonomous driving. In: The Fourteenth International Conference on Learning Representations (18 Dec 2025). https://doi.org/10.48550/arXiv.2510.12796, https://openreview.net/pdf/bdeb32be26f4458b09aff185a33416fb7cf4c689.pdf 2, 4, 5
9. Mao, J., Qian, Y., Ye, J., Zhao, H., Wang, Y.: GPT-Driver: Learning to Drive with GPT. In: NeurIPS 2023 Foundation Models for Decision Making Workshop (2 Oct 2023), http://arxiv.org/abs/2310.01415 4
10. Mao, J., Ye, J., Qian, Y., Pavone, M., Wang, Y.: A language agent for autonomous driving. In: Conference on Language Modeling (7 Oct 2024) 4
11. Physical Intelligence, Black, K., Brown, N., Darpinian, J., Dhabalia, K., Driess, D., Esmail, A., Equi, M., Finn, C., Fusai, N., Galliker, M.Y., Ghosh, D., Groom, L., Hausman, K., Ichter, B., Jakubczak, S., Jones, T., Ke, L., LeBlanc, D., Levine, S., Li-Bell, A., Mothukuri, M., Nair, S., Pertsch, K., Ren, A.Z., Shi, L.X., Smith, L., Springenberg, J.T., Stachowicz, K., Tanner, J., Vuong, Q., Walke, H., Walling, A., Wang, H., Yu, L., Zhilinsky, U.: $\pi_{0.5}$: A vision-language-action model with open-world generalization. arXiv [cs.LG] (22 Apr 2025). https://doi.org/10.48550/arXiv.2504.16054, http://arxiv.org/abs/2504.16054 4
12. Prakash, A., Chitta, K., Geiger, A.: Multi-modal fusion transformer for end-to-end autonomous driving. In: 2021 IEEE/CVF Conference on Computer Vision and Pattern Recognition (CVPR). pp. 7073–7083. IEEE (Jun 2021). https://doi.org/10.1109/cvpr46437.2021.00700, http://dx.doi.org/10.1109/CVPR46437.2021.00700 4
13. Ramstedt, S., Pal, C.: Real-Time Reinforcement Learning. arXiv [cs.LG] (11 Nov 2019). https://doi.org/10.48550/arXiv.1911.04448, http://arxiv.org/abs/1911.04448 5
14. Renz, K., Chen, L., Arani, E., Sinavski, O.: SimLingo: Vision-Only Closed-Loop Autonomous Driving with Language-Action Alignment. In: Proceedings of the IEEE/CVF Conference on Computer Vision and Pattern Recognition. pp. 11993–12003. openaccess.thecvf.com (2025), http://openaccess.thecvf.com/content/CVPR2025/html/Renz_SimLingo_Vision-Only_Closed-Loop_Autonomous_Driving_with_Language-Action_Alignment_CVPR_2025_paper.html 4
15. Renz, K., Chen, L., Marcu, A.M., Hünermann, J., Hanotte, B., Karnsund, A., Shotton, J., Arani, E., Sinavski, O.: CarLLaVA: Vision language models for camera-only

closed-loop driving. In: 2024 Conference on Computer Vision and Pattern Recognition (14 Jun 2024) 4
16. Shao, H., Hu, Y., Wang, L., Waslander, S.L., Liu, Y., Li, H.: LMDrive: Closed-Loop End-to-End Driving with Large Language Models. In: Proceedings of the IEEE/CVF Conference on Computer Vision and Pattern Recognition (2024), http://arxiv.org/abs/2312.07488 2, 4, 5
17. Shao, H., Wang, L., Chen, R., Li, H., Liu, Y.: Safety-Enhanced Autonomous Driving Using Interpretable Sensor Fusion Transformer. In: Liu, K., Kulic, D., Ichnowski, J. (eds.) Proceedings of The 6th Conference on Robot Learning. Proceedings of Machine Learning Research, vol. 205, pp. 726–737. PMLR (2023), https://proceedings.mlr.press/v205/shao23a.html 4
18. Shao, H., Wang, L., Chen, R., Waslander, S.L., Li, H., Liu, Y.: ReasonNet: End-to-end driving with temporal and global reasoning. arXiv [cs.CV] (17 May 2023). https://doi.org/10.48550/arXiv.2305.10507, http://arxiv.org/abs/2305.10507 4
19. Sima, C., Renz, K., Chitta, K., Chen, L., Zhang, H., Xie, C., Luo, P., Geiger, A., Li, H.: DriveLM: Driving with graph visual question answering. In: European Conference on Computer Vision 2024 (29 Sep 2024) 2, 4
20. Tian, X., Gu, J., Li, B., Liu, Y., Wang, Y., Zhao, Z., Zhan, K., Jia, P., Lang, X., Zhao, H.: DriveVLM: The Convergence of Autonomous Driving and Large Vision-Language Models. In: 8th Annual Conference on Robot Learning (5 Sep 2024), https://openreview.net/pdf?id=928V4Umlys 2, 4
21. Touvron, H., Lavril, T., Izacard, G., Martinet, X., Lachaux, M.A., Lacroix, T., Rozière, B., Goyal, N., Hambro, E., Azhar, F., Rodriguez, A., Joulin, A., Grave, E., Lample, G.: LLaMA: Open and efficient foundation language models. arXiv [cs.CL] (27 Feb 2023), http://arxiv.org/abs/2302.13971 5
22. Wu, P., Jia, X., Chen, L., Yan, J., Li, H., Qiao, Y.: Trajectory-guided control prediction for end-to-end autonomous driving: A simple yet strong baseline. In: Advances in Neural Information Processing Systems 35. pp. 6119–6132. Neural Information Processing Systems Foundation, Inc. (NeurIPS), San Diego, California, USA (2022). https://doi.org/10.52202/068431-0443, http://dx.doi.org/10.5555/3600270.3600713 4
23. Xiao, T., Jang, E., Kalashnikov, D., Levine, S., Ibarz, J., Hausman, K., Herzog, A.: Thinking While Moving: Deep Reinforcement Learning with Concurrent Control. In: International Conference on Learning Representations (25 Sep 2019), https://openreview.net/forum?id=SJexHkSFPS 5
24. Xu, Z., Zhang, Y., Xie, E., Zhao, Z., Guo, Y., Wong, K.Y.K., Li, Z., Zhao, H.: DriveGPT4: Interpretable end-to-end autonomous driving via large language model. IEEE Robot. Autom. Lett. **9**(10), 8186–8193 (Oct 2024). https://doi.org/10.1109/lra.2024.3440097 2, 4
25. Zhao, T.Z., Kumar, V., Levine, S., Finn, C.: Learning fine-grained bimanual manipulation with low-cost hardware. arXiv [cs.RO] (23 Apr 2023). https://doi.org/10.48550/arXiv.2304.13705, http://arxiv.org/abs/2304.13705 4